remote sensing

MDPI

Article

Spatial and Temporal Dynamics of Transportation Accessibility in China: Insights from Sustainable Development Goal Indicators from 2015 to 2022

Minshu Yang [1], Zhongchang Sun [2,3,*], Xiaoying Ouyang [2,3], Hongwei Li [2,3], Youmei Han [1] and Dinoo Gunasekera [2,3]

[1] School of Marine Technology and Geomatics, Jiangsu Ocean University, Lianyungang 222005, China; 2022220251@jou.edu.cn (M.Y.)
[2] International Research Center of Big Data for Sustainable Development Goals (CBAS), Beijing 100094, China
[3] Key Laboratory of Digital Earth Science, Aerospace Information Research Institute (AIR), Chinese Academy of Sciences (CAS), Beijing 100094, China
* Correspondence: sunzc@aircas.ac.cn

Abstract: SDG 9.1.1 and SDG 11.2.1 are significant evaluation indicators of the United Nations Sustainable Development Goals related to transportation accessibility and are used to measure the proportion of the population facilitating the use of road services in rural areas and the proportion of the population facilitating the use of public transportation services in urban areas, respectively. However, there are currently challenges related to incomplete data and the inadequate interpretation of the indicators. In this study, we therefore evaluate the spatiotemporal patterns of the indicators and the number of disadvantaged groups in 337 Chinese cities from 2015 to 2022 based on multi-source data, and explore the spatial aggregation of the indicators and the driving factors. The results demonstrate that the indicator values of SDG 9.1.1 and SDG 11.2.1 reached 99.36% and 90.00%, respectively, in 2022, and the number of vulnerable groups decreased to approximately 1.89 million and 2.82 million. The indicator values of SDG 9.1.1 are high in the eastern part of China and low in the western part of the country, whereas the indicator values of SDG 11.2.1 exhibit spatial agglomeration in regions such as the Pearl River Delta. The average rural elevation and the density of urban public transportation stops are the most influential factors for these two indicators, respectively. The insights and data from this study provide support for improving transportation infrastructure and inequality in China, contributing to the achievement of the 2030 Sustainable Development Goals.

Keywords: sustainable development goals (SDGs); transportation accessibility; SDG 9.1.1; SDG 11.2.1; spatial and temporal patterns

check for updates

Citation: Yang, M.; Sun, Z.; Ouyang, X.; Li, H.; Han, Y.; Gunasekera, D. Spatial and Temporal Dynamics of Transportation Accessibility in China: Insights from Sustainable Development Goal Indicators from 2015 to 2022. *Remote Sens.* **2024**, *16*, 4452. https://doi.org/10.3390/rs16234452

Academic Editor: Yuji Murayama

Received: 28 October 2024
Revised: 25 November 2024
Accepted: 25 November 2024
Published: 27 November 2024

Copyright: © 2024 by the authors. Licensee MDPI, Basel, Switzerland. This article is an open access article distributed under the terms and conditions of the Creative Commons Attribution (CC BY) license (https://creativecommons.org/licenses/by/4.0/).

1. Introduction

With the rapid development of society, transportation accessibility has become an important determinant of socio-economic development and regional connectivity [1,2]. The global indicator framework of the 2030 Agenda for Sustainable Development clearly indicates the importance of transportation accessibility [3–6], with SDG9.1.1 (proportion of the rural population who lived within 2 km of an all-season road) focusing on improving the accessibility of road infrastructure in rural areas, and SDG11.2.1 (proportion of the urban population that had convenient access to public transport) looking at the convenience and accessibility of urban public transportation systems [7–9].

Many studies have explored the status and trends in SDG 9.1.1 and SDG 11.2.1 at different spatial scales [10,11]. Internationally, rural road accessibility in countries such as Uganda and Armenia has been studied through national road networks and population data [12–14]. In Algeria, the impact of highway projects under the Belt and Road Initiative on accessibility and economic development was examined [15,16]. By 2020, more than 60%

of the population of the world's major cities had easy access to public transportation [17], while only one-third of the population in the African region had easy access to public transportation [18]. Researchers assessed road accessibility in rural areas across counties in China in 2017 [19], revealing the distribution of transportation services and the extent of improvement. Meanwhile, SDG 11.2.1 indicator values for China increased from 2015 to 2020 [20,21], and some researchers also explored the SDG 11.2.1 indicator for Guilin at the municipal scale [22]. Although many studies have explored transportation accessibility in relation to the SDG 9.1.1 and SDG 11.2.1 indicators [23], there are few valid data references on the spatial and temporal dynamic patterns of indicator development in cities across the country. Moreover, the uneven and unequal development of transportation accessibility across the country remains particularly problematic [24,25].

Transportation accessibility, as an important comprehensive indicator for evaluating transportation networks and locations, not only reflects the spatial characteristics of an area but also has an important impact on the socio-economic status and lifestyle of residents [26]. The traditional method of measuring rural road accessibility was mainly based on household survey calculations, but this was costly and did not facilitate spatial analysis or regular updates [27]. In 2016, the World Bank proposed a new method of measuring rural road accessibility using buffer zones. This method, based on multi-source data [7], allowed rural road accessibility to be assessed through spatial buffer analysis and superposition analysis [28]. On the other hand, there were many research methods for measuring the accessibility of urban public transportation [29], mainly in the following categories: creating buffer zones to determine accessibility based on the location of public transportation stations, which was convenient to operate but did not give enough consideration to the actual travel situation [30]; analyzing the accessibility of public transportation by measuring the supply and demand relationship between origins and destinations, which reasonably reflected the spatial variability of supply and demand but whose indicator values lacked specific practical significance [31]; the network analysis method that focused on the actual public transportation travel paths and studied the various impediments encountered in the travel process, which fully took into account the actual public transportation routes but was complicated to operate and did not consider the actual travel demand [32–34]; the transformation of urban spatial vector elements into raster data for the weighted computation of travel cost, which was mainly used for the presentation of point accessibility but was complicated to compute and difficult to operate [35,36]; and high-precision public transportation accessibility analysis based on open map APIs, which considered the whole process of public transportation travel but required capturing and processing large amounts of data [37]. Given that the purpose of SDG 9.1.1 and SDG 11.2.1 was to calculate a population ratio, and a range was needed to determine the population number with the help of population grid data [38], the buffer zone method, which is simpler to operate and applicable to a large range of calculations, was more suitable for this study. Simultaneously, traditional calculations were typically processed using GIS software [39], but its local computing capabilities limit its ability to handle large-scale calculations. The powerful capabilities of the Google Earth Engine (GEE) platform in geographic information analysis and spatial data processing provide significant technical support for the study of sustainable transport [40–43].

The values of the two indicators related to transport accessibility were only expressed as proportional data. However, one of the core concepts of the SDGs was that no one should be left behind, and proportional values alone did not provide a full picture of the specific number of people in municipalities who were truly facing inconvenience in accessing transport services [23]. The SDG 9.1.1 and SDG 11.2.1 indicators could have been supplemented by calculating the number of people in the transport-disadvantaged group who did not have convenient access to roads and public transportation. In addition, according to the first law of geography [44], "Everything is related to everything else, and what is near is more related than what is far", after calculating the relevant indicator values for each city in the country, the existence of regional aggregation of indicator values in

neighboring cities still needed further exploration [45]. Moreover, the factors driving the changes in these indicators also needed to be clarified [46,47].

In this study, our analysis aims to provide data support and scientific basis for optimizing resource allocation and solving the problem of transportation inequality in China [6], and we explore the following four questions: (1) What was the spatiotemporal pattern of the two indicators, SDG 9.1.1 and SDG 11.2.1, in the 337 municipalities across the country? (2) What was the number of people who did not have easy access to roads in rural areas and to public transportation in urban areas, and how was it distributed? (3) Was there a clustering or dispersion phenomenon of the two indicators, SDG 9.1.1 and SDG 11.2.1, across the country? (4) What were the impact factors of the two indicators, SDG 9.1.1 and SDG 11.2.1?

2. Study Areas and Datasets

2.1. Study Areas

According to the 2020 Statistical Bulletin on the Development of Civil Affairs from the Ministry of Civil Affairs of China, as of the end of 2020 [48], there were four municipalities directly under the central government and 333 prefectural-level administrative units (including 293 prefectural-level municipalities, 30 autonomous prefectures, 3 leagues, and 7 districts) in the country. These 337 municipalities were selected as the study area (Figure 1). As one of the most populous countries in the world, most of China's population is clustered in the southeast region of the Hu Huanyong Line, a region that includes economically developed and densely populated areas such as the Yangtze River Delta region and the Pearl River Delta. China's topography is characterized by a high west and a low east, with the west including areas with complex landscapes such as the Tibetan Plateau and the Western Sichuan Plateau, while the eastern region includes flatter areas such as the North China Plain and the Yangtze River Basin.

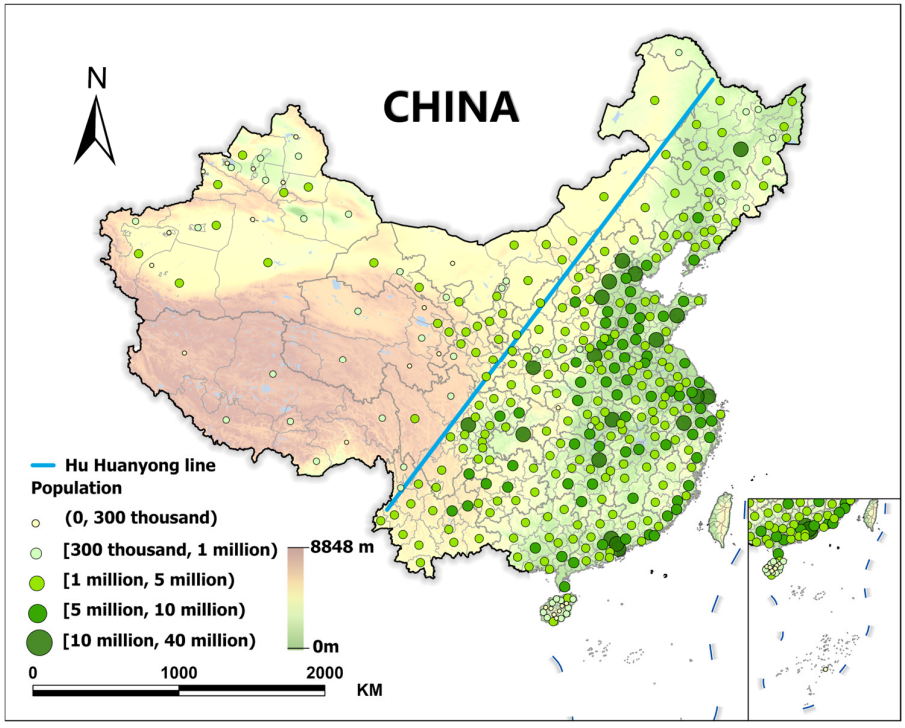


Figure 1. Elevation and population distribution of China in 2022.

2.2. Datasets

This study used a variety of geographical and socio-economic data (Table 1). As 2023 was the United Nations mid-term evaluation year for sustainable development [49], three time points were selected for the analysis: 2015, 2020, and 2022.

Table 1. Datasets used in our study.

Data Name	Data Source	Year
Road Network Data	National Catalogue Service for Geographic Information (https://www.webmap.cn/ (accessed on 26 June 2024)) Amap (https://lbs.amap.com/ (accessed on 28 June 2024))	2015, 2017, 2020, 2022
Bus Stop Data	Amap (https://lbs.amap.com/ (accessed on 28 June 2024))	2015, 2020, 2022
Subway Station Data	Amap (https://lbs.amap.com/ (accessed on 28 June 2024))	2015, 2020, 2022
Population Grid Data	Landscan (https://landscan.ornl.gov/ (accessed on 28 June 2024))	2015, 2020, 2022
Urban Built-up Area Data	http://www.doi.org/10.11922/sciencedb.j00076.00004 (accessed on 28 June 2024)	2015, 2020
Administrative Boundaries	National Catalogue Service For Geographic Information (https://www.webmap.cn/ (accessed on 28 June 2024))	2022
GDP Data	Nation Bureau of Statistics (https://www.stats.gov.cn/ (accessed on 29 June 2024))	2020
SRTM Digital Elevation Data	GEE Platform	2020
Population Data	Nation Bureau of Statistics (https://www.stats.gov.cn/ (accessed on 29 June 2024))	2020
Impervious Surface Data	International Research Center of Big Data for Sustainable Development Goals	2015, 2018, 2021

2.3. Data Preprocessing

The road network data for 2020 and 2022 contained some missing roads at the village level; thus, the data for these two years were overlaid and analyzed with the 2017 road data from the National Catalogue Service for Geographic Information to obtain the national road data for 2020 and 2022. The 2015 data were taken directly from the National Catalogue Service for Geographic Information road data. Considering the closed characteristics of highways and elevated roads (because highways and elevated roads are open or closed depending on the weather, for example, they are closed and open during severe weather such as fog, so these roads are not considered as four-season access roads), only road types such as national highways, provincial highways, county highways, township roads, and other highways were considered as all-season access roads in this study.

For the public transport station points of interest (POIs) data crawled by Amap, data cleaning and coordinate correction were performed to generate the national public transport station data for three years, 2015, 2020, and 2022. As the built-up area data for 2022 were missing, the 2020 data were used as a substitute in the subsequent study [50,51]. Simultaneously, based on the underlying data presented in Table 1, auxiliary data were produced to explore the influence of socio-economic and geographical environmental factors on the indicators using multi-scale geographically weighted regression models. These data included the population data of each city to calculate the urban and rural population density on the GEE platform, the public transport station data divided by the built-up area to calculate the public transport station density, the Shutter Radar Topography Mission (SRTM) digital elevation data to calculate the mean elevation and standard deviation of the slope for each city, and the road network data to calculate the road density of each city and the rural area on the GEE platform.

3. Methodology

In this study, we calculated the two indicator values and the number of vulnerable groups using the GEE platform. In the overlay analysis for calculating the population counts, we used an area-weighting method to minimize errors caused by the incomplete overlap of administrative areas and demographic grid data when calculating the population counts. In addition, we explored the spatial aggregation of the indicators and the factors influencing them using the Moran Index and multi-scale geographically weighted regression models.

3.1. Methodology for the Calculation of Indicators SDG 9.1.1 and SDG 11.2.1

The SDG 9.1.1 indicator measured the proportion of the rural population who lived within 2 km of an all-season road using the following formula:

$$\text{SDG9.1.1} = \frac{\text{POP}_{served9}}{\text{POP}_{rural}} \times 100\% \quad (1)$$

where

- POP_{rural} denotes the total population in rural areas (calculated by overlaying rural areas with population data).
- $\text{POP}_{served9}$ denotes the total rural population living within 2 km of an all-season road (calculated by overlaying road buffer zones with population data).
- SDG 9.1.1 takes values between 0% and 100%, where 100% means that all rural populations live within 2 km of an all-season road, and 0% means that all rural populations live outside 2 km of an all-season road.

The SDG 11.2.1 indicator measured the proportion of the population that had convenient access to public transport using the following formula:

$$\text{SDG11.2.1} = \frac{\text{POP}_{served11}}{\text{POP}_{urban}} \times 100\% \quad (2)$$

where

- POP_{urban} denotes the total population of the urban area (obtained by overlaying urban areas with population data).
- $\text{POP}_{served11}$ denotes the total urban population living in an area where public transportation was easily accessible, with reference to the official definition (obtained by overlaying station buffers with population data).
- SDG 11.2.1 takes values between 0% and 100%, with 100% indicating that all urban populations can easily access public transportation within a certain range, and 0% indicating that none can easily access public transportation.

3.2. Automatic Extraction of Indicators Based on GEE

This study adopted the GEE platform to calculate indicator data. Some research data could not be obtained directly online, hence processed datasets were uploaded to the GEE platform for subsequent operations (Figure 2).

The classification of urban and rural areas was controversial due to the lack of common standards. To differentiate between urban and rural areas in the study, administrative district data and built-up area data were overlaid and analyzed [52]. The division between urban and rural areas was based on whether the area was within a built-up area.

Based on the processed national all-season road data, a 2 km radius buffer zone was created and overlaid on the rural area to obtain the rural road buffer zone data. Since bus stops and metro stations may have different passenger flows, a buffer zone of 500 m for bus stops and 1000 m for metro stations was created based on the processed national public transport station data and overlaid with the urban area to obtain the urban public transport station buffer zone. Rural road buffers, urban public transport station buffers, urban areas,

and rural areas were overlaid with population data to calculate the population size of each area. The number of people in the buffer zone of rural all-season roads was calculated and analyzed with the number of people in rural areas to obtain the indicator number for SDG 9.1.1. Similarly, the number of people in the buffer zone of urban public transport stations was calculated and analyzed with the number of people in urban areas to obtain the indicator number for SDG 11.2.1.

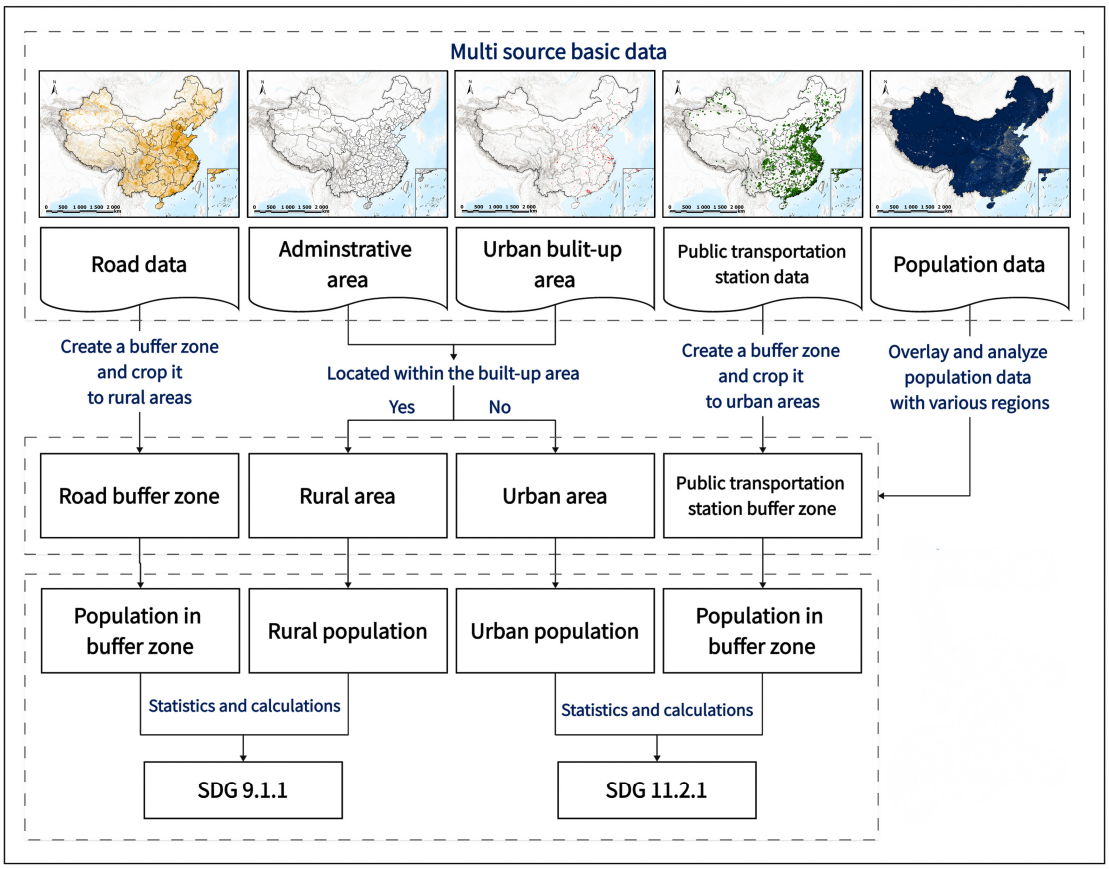


Figure 2. Metrics processing flow in the GEE platform.

Since LandScan data are raster data with a resolution of 1 km, and built-up areas or buffer zones are vector data, some pixels in the edge areas were not fully included in the built-up areas or buffer zones when performing population overlay calculations, thus reducing the accuracy of the calculations. Traditional GIS methods for zoning statistics usually use the pixel-centered method to determine whether an image element is within a vector area. This method creates small image elements based on large image elements, and if the center of a small image element falls within the vector area, the image element is considered to belong entirely to the vector area. This method does not take into account the actual population distribution within the image element and thus may produce large errors.

In this study, an improved method was used to calculate the population data within the vector region. The specific steps were as follows. The image elements were divided into two categories: image elements completely contained within the vector region and image elements intersecting the vector region. For image elements completely contained within the vector region, the representative population data of the image elements were directly used; for image elements intersecting the vector region, the impervious surface data were used to determine the human settlement area and calculate the portion of its population contained within the vector region.

The specific calculations were as follows: For an image element that was completely contained within the vector region, its population number P_{total} was used directly. For

image elements intersecting the vector region, their population number P_{region} in the human settlement area was calculated as follows:

$$P_{region} = P_{total} \times \frac{A_{inter}}{A_{pixel}} \quad (3)$$

Ultimately, the total population number P_{total_region} within the vector region was the sum of the population number $P_{complete}$ of the fully contained image element and the population number P_{region} of the intersecting image element:

$$P_{total_region} = \sum P_{complete} + \sum P_{region} \quad (4)$$

where

- P_{total} is the number of people represented by that image element.
- A_{inter} is the impervious area in the image element that intersects the vector region.
- A_{pixel} is the impervious area of the image element.
- P_{region} is the population number in the image element with incomplete containment within the vector region.
- $P_{complete}$ is the population number in the image element with complete inclusion.
- P_{total_region} is the total population in the vector region.

By this method, the population number within the vector region could be estimated more accurately, thus improving the accuracy of the population overlay calculation.

3.3. Moran's Index

In order to investigate whether the indicator values of SDG 9.1.1 and SDG 11.2.1 are clustered at the national level, Moran's Index I (Moran's Index) was used for validation. Moran's I is a statistical tool used to measure autocorrelation of geospatial data and is categorized into Global Moran's I and Local Moran's I [53]. Global Moran's I assessed the spatial autocorrelation of the indicators and evaluated the significance of the overall spatial pattern using metrics such as Moran's Index, z-scores, and *p*-values. These metrics reflected whether the eigenvalues across the study area tended to be similar (positive autocorrelation) or dissimilar (negative autocorrelation). Local Moran's I assessed four patterns of spatial autocorrelation at specific local locations: high–high clustering, low–low clustering, high–low outliers, and low–high outliers [54].

3.4. Multi-Scale Geographically Weighted Models

A multi-scale geographically weighted regression (MGWR) model was used to explore the impact of socio-economic and geo-environmental factors on changes in the SDG 9.1.1 and SDG 11.2.1 indicators [45]. The model employed personalized spatial modeling to improve the accuracy and explanatory power of the spatial process model by assigning different levels of spatial smoothing and optimal bandwidths to each covariate. In MGWR, the golden search algorithm could be used to find the most appropriate bandwidths for different variables, thus performing regression modeling that avoided the mismatch between the bandwidths and the scales of action of the variables, reducing the noise in parameter estimation. The formula for the model is as follows:

$$y_i = \sum_{j=1}^{k} \beta_{bwj}(u_i, v_i)_{x_{ij}} + \varepsilon_i \quad (5)$$

where

- bwj represents the bandwidth used for the regression coefficients of the variable.
- y_i denotes the indicator value of the municipality.
- x_{ij} denotes the built environment in the grid.
- (u_i,v_i) denotes the center of mass coordinates of the municipality.
- β_{bwj} denotes the regression coefficients of the variable in the grid under bandwidth.

- k denotes the number of samples.
- ε_i denotes the random error term.

4. Results and Analysis

4.1. Characterization of Spatial and Temporal Patterns

4.1.1. Overall Status of Indicators

Overall, both the SDG 9.1.1 and SDG 11.2.1 indicators demonstrate an upward trend (Figure 3). The national averages for the SDG 9.1.1 indicator for the years 2015, 2020, and 2022 were 98.68%, 99.03%, and 99.36%, respectively, showing a total increase of 0.68% from 2015 to 2022. The number of municipalities where the SDG 9.1.1 indicator did not exceed 90% decreased from 10 in 2015 to 1 in 2022. The national averages for the SDG 11.2.1 indicator for the years 2015, 2020, and 2022 were 85.15%, 88.34%, and 90.00%, respectively, with a total improvement of 4.85% from 2015 to 2022. The proportion of municipalities that reached 90% for the SDG 11.2.1 indicator was 17.5% in 2015, 30.6% in 2020, and 39.1% in 2022.

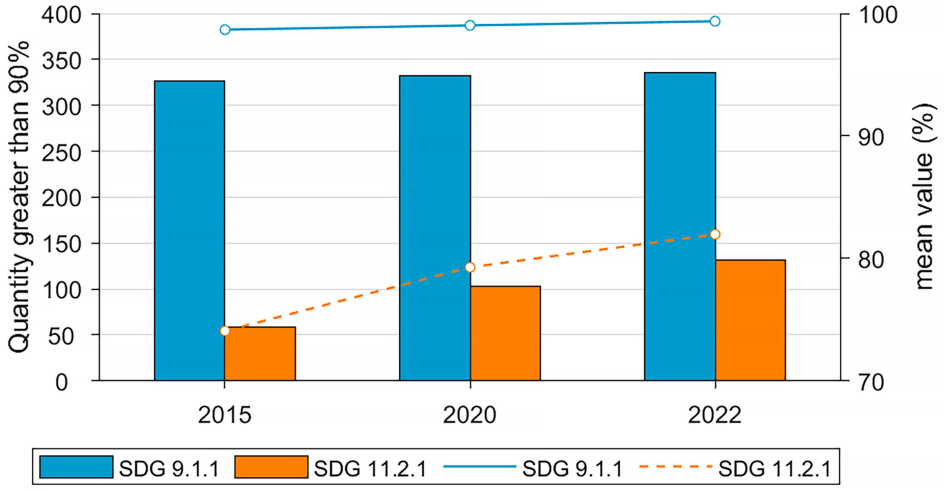


Figure 3. Number of cities with indicator scores above 90% for SDG 9.1.1 and SDG 11.2.1 and the national average. The bar chart shows the number of cities with indicators above 90%, and the line chart shows the national average of the indicators.

4.1.2. Characterization of Spatial Patterns of Indicators

The spatial patterns of SDG 9.1.1 and SDG 11.2.1 indicators over different years reveal significant spatial heterogeneity (Figure 4). In 2015, the SDG 9.1.1 indicator values were higher in the east and lower in the west (Figure 4a), consistent with the geographical characteristics of the Hu Huanyong Line. A total of 13 municipalities in northwestern Yunnan, western Qinghai, northwestern Sichuan, and northern Tibet failed to reach 90% of the SDG 9.1.1 indicator value, primarily due to harsh geographical environments such as plateaus and deserts, which complicate and increase the cost of road infrastructure construction. By 2020 (Figure 4b), the SDG 9.1.1 indicator values of Linzhi and Shannan in Xizang and Yunnan Province had all risen above 90%. By 2022 (Figure 4c), all Chinese municipalities except Ngari Prefecture had indicator values exceeding 95%, reflecting significant achievements in rural infrastructure construction in China.

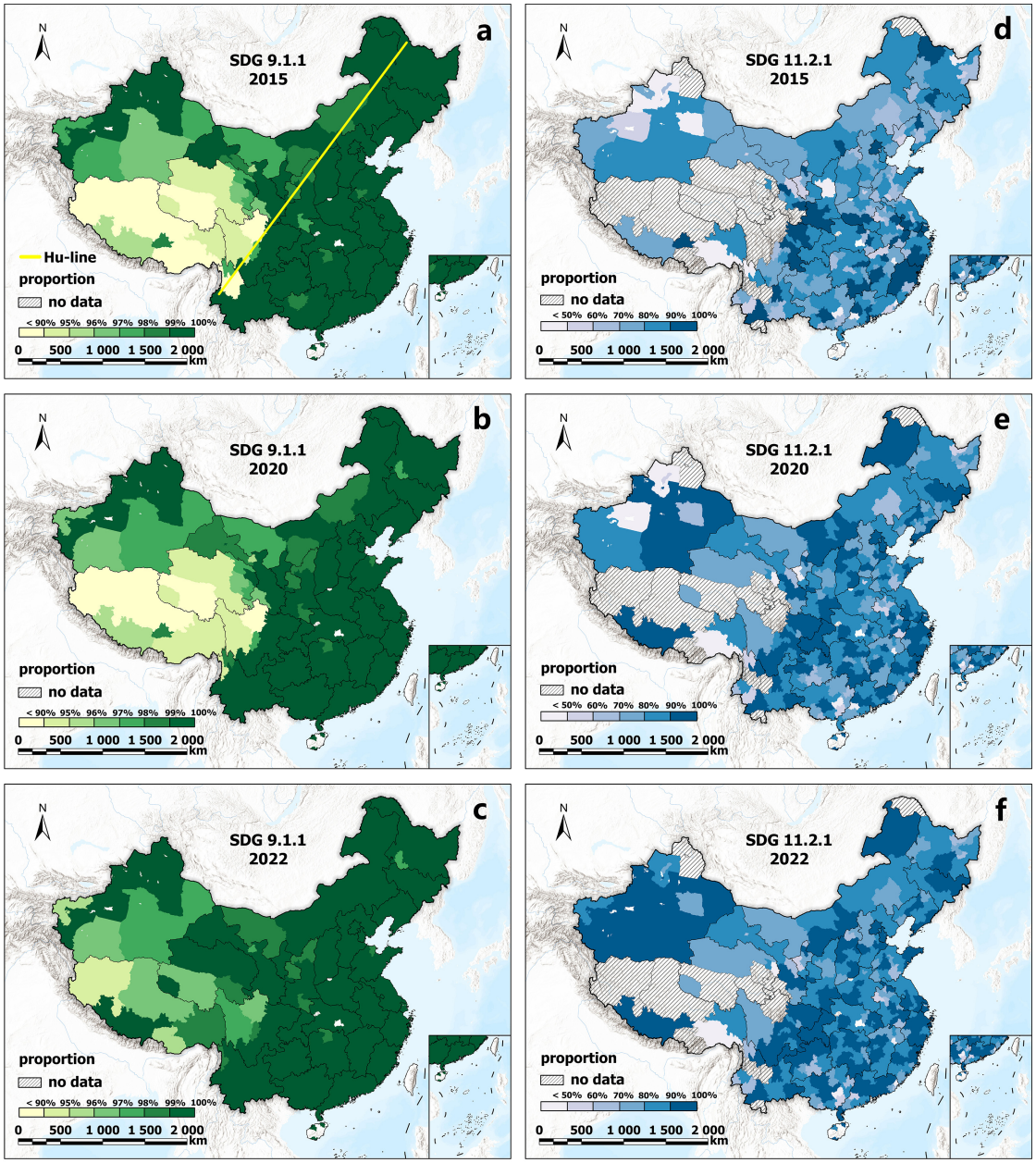


Figure 4. Spatial patterns for indicators, (**a**) shows the spatial distribution of SDG 9.1.1 2015; (**b**) shows the spatial distribution of SDG 9.1.1 2020; (**c**) shows the spatial distribution of SDG 9.1.1 2022; (**d**) shows the spatial distribution of SDG 11.2.1 2015; (**e**) shows the spatial distribution of SDG 11.2.1 2020; (**f**) shows the spatial distribution of SDG 11.2.1 spatial distribution for 2022.

The 2015 SDG 11.2.1 indicator data (Figure 4d) were more dispersed, with the southeast coast, Chengdu, the Xi'an region, and the Yangtze River Delta around Shanghai having significantly higher values than other regions, reaching over 90%. By 2022 (Figure 4f), nine cities in the Xinjiang region, as well as cities in northern Guizhou, southern Sichuan, and Chongqing had all reached 90%. In western China, regions such as Lhasa and Shigatse had higher indicator scores due to their relatively small built-up areas, where fewer public transport stations could cover the entire city. However, in 2022, regions such as northern Inner Mongolia, the northeast, Gansu, and Qinghai had an average indicator value of around 75%.

4.1.3. Characterization of the Time Pattern of Indicators

From 2015 to 2022, the SDG 9.1.1 indicator exhibited positive development, with 66.5% of the country's 337 municipalities experiencing growth (Figure 5a). The highest growth rate was observed in Nujiang Lisu Autonomous Prefecture in Yunnan Province, with a 43.48% increase. Nine cities with growth rates of 10% or more were located in Sichuan, Tibet, Qinghai, and Yunnan. Despite this progress, 113 municipalities still experienced a decline, mostly less than 0.1%. The declining cities were mainly concentrated in the southeast of the Hu Huanyong Line, where the indicator value had reached over 99% in 15 years. This decline is attributed to the slower rate of rural population decline compared to the urbanization rate. However, overall, the proportion of decline was relatively low, while the declining areas still maintained a high proportion value, and the overall impact was low.

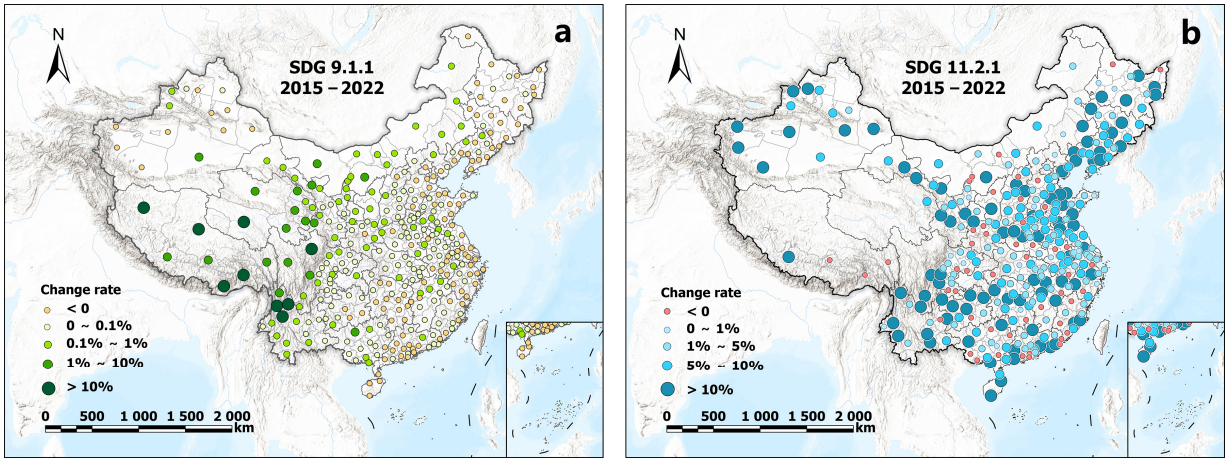


Figure 5. Changes in SDG 9.1.1 and SDG 11.2.1 indicators from 2015 to 2022. (**a**) shows changes in SDG 9.1.1 indicators and (**b**) shows changes in SDG 11.2.1 indicators.

For the SDG 11.2.1 indicator, after removing 22 cities with missing 2015 data, 266 cities showed an increase from 2015 to 2022, with 93 cities experiencing growth rates of 10% or more (Figure 5b). The Asku region had the highest growth rate of 40.60%, indicating that these regions had seen the first results of their investment in public transport in recent years. A total of 49 cities exhibited decreases, with 34 showing decreases of less than 5 percent, primarily in the southeast of the Hu Huanyong Line due to factors such as the rapid expansion of built-up areas, population movement, and the irrationality of new development.

4.2. Analysis of Temporal and Spatial Patterns of Indicator Vulnerable Populations

The number of rural residents without easy road access dropped from 3.95 million in 2015 to 1.89 million in 2022, a 52% decrease. These populations were primarily in southern Xinjiang, northern Sichuan, northern Heilongjiang, northern Hunan, and northern Shaanxi (Figure 6a). Notably, Chongqing Municipality led in the number of inconvenienced people due to its complex topography. The urban population without easy public transport decreased from about 3.78 million in 2015 to about 2.82 million in 2022, a 25.3% decrease (Figure 6b). The majority were in densely populated areas east of the Hu Huanyong Line, where localized gaps in public transport coverage left many without easy access.

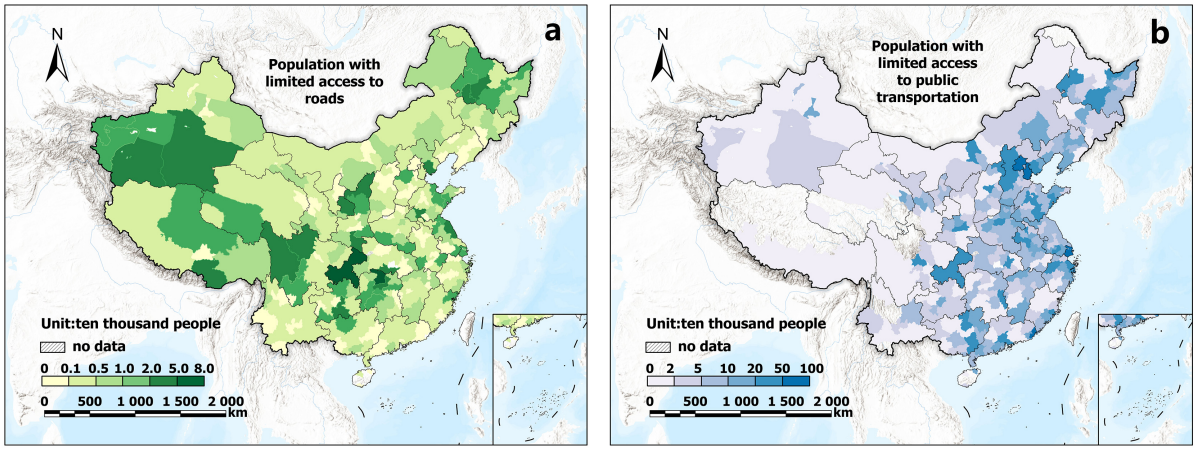


Figure 6. Spatial distribution of population with inconvenient access to roads and public transportation in 2022. (**a**) shows the distribution of the population with poor access to roads and (**b**) shows the distribution of the population with poor access to public transportation.

4.3. Spatial Autocorrelation Analysis

This study identified spatial aggregation in the SDG 9.1.1 and SDG 11.2.1 indicators. Moran's Index was used to explore the spatial autocorrelation of the 2020 indicator scores at the national level. The global Moran's Index (Table 2) for SDG 9.1.1 was approximately 0.364, indicating significant positive spatial autocorrelation and a clustering trend in the data values. The indicator had a z-score of approximately 15.088 and a *p*-value of 0, indicating that this pattern of aggregation was statistically significant. The SDG 11.2.1 indicator also showed positive spatial autocorrelation, with a Moran's Index of around 0.088, but with a lesser degree of spatial aggregation, with a corresponding z-score of around 3.506 and a *p*-value of 0.001, suggesting that its spatial aggregation existed but was not as strong as that of the SDG 9.1.1 indicator.

Table 2. Global Moran Index results for 2020.

	Moran's Index	Expected Index	Variance	z-Score	*p*-Value
SDG 9.1.1	0.364	−0.003	0.001	15.088	0.000
SDG 11.2.1	0.088	−0.003	0.001	3.506	0.001

The local Moran's Index for SDG 9.1.1 exhibited high values in the east and low values in the west, with significant positive autocorrelation in coastal provinces (Figure 7c). Western China, including Tibet, Qinghai, and parts of Sichuan and Xinjiang, was a cold spot with significantly lower indicator values (Figure 7e). The SDG 11.2.1 indicator showed high aggregation in the Sichuan–Chongqing, Yangtze River Delta, and Pearl River Delta regions, with more dispersed low aggregation in Tibet, Qinghai, Sichuan, Guangxi, Jiangxi, and northern Anhui (Figure 7d,e). The scatter plot of the local Moran's Index showed that the SDG 9.1.1 indicator accounted for more municipalities with high–high-type aggregation, indicating that the SDG 9.1.1 indicator had a strong spatial positive correlation and significant spatial clustering characteristics at the national level. SDG 11.2.1 (Figure 7a,b), on the other hand, was more dispersed, with more municipalities clustered in low–low and high–high types than in high–low and low–high types.

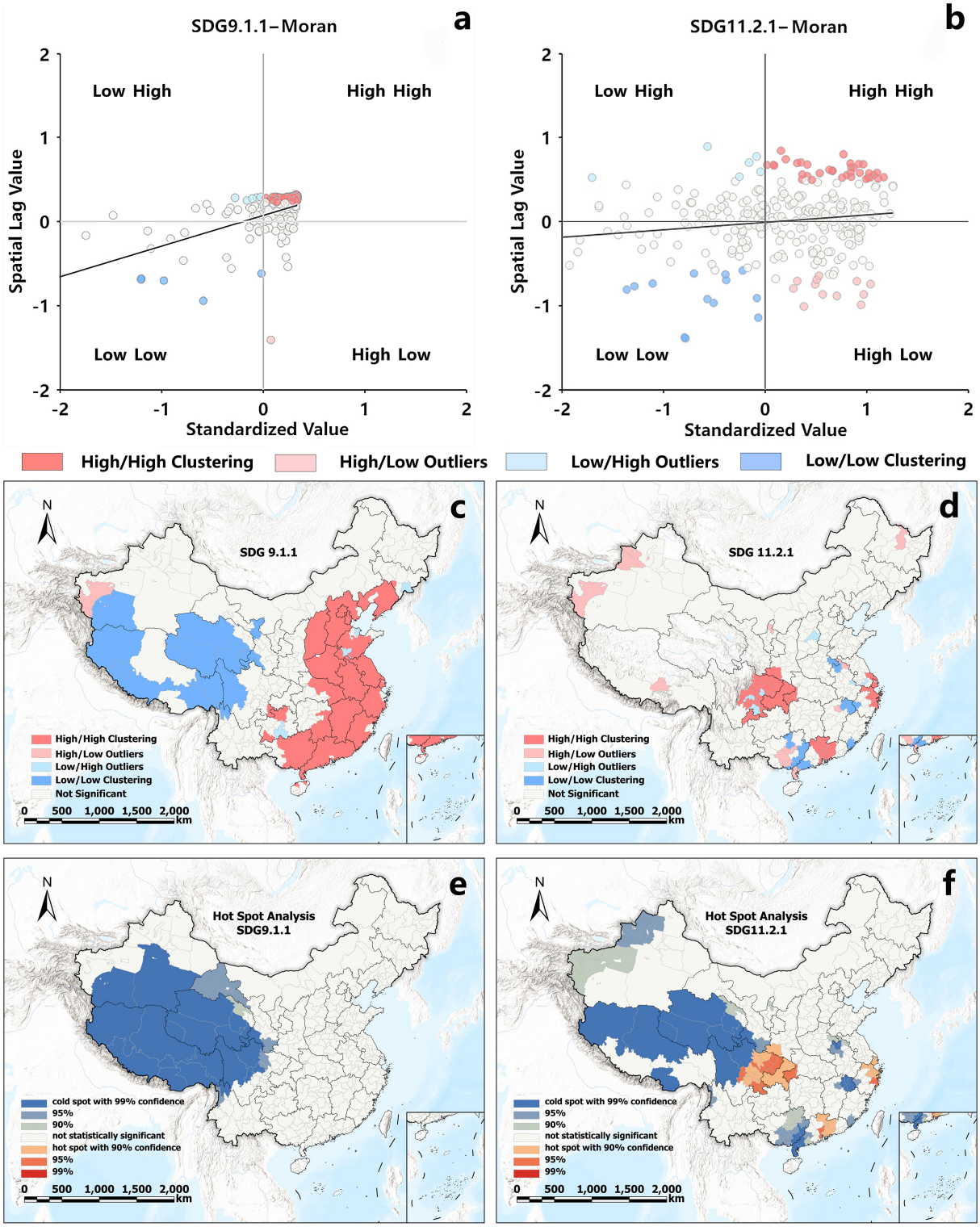


Figure 7. Localized Moran's Index results for 2020. (**a**,**b**) show scatter plots of the localized Moran's Index; (**c**,**d**) show spatial distribution patterns of the localized Moran's Index; (**e**,**f**) show hot and cold spot analyses of the localized Moran's Index.

4.4. Analysis of Influencing Factors

This paper analyzes the spatial patterns of China's SDG 9.1.1 and SDG 11.2.1 indicators in terms of socio-economic and topographic variables. Studies have shown that the degree of rural road access in China is closely related to economic development and topographic features. Therefore, this paper selects municipal population, population density, and GDP

data as well as road and station density data as socio-economic explanatory variables and calculates them based on relevant data. Meanwhile, considering the influence of topographic factors, this paper introduces mean elevation and slope standard deviation as topographic variables, and constructs multi-scale geographically weighted regression (MGWR) models for SDG 9.1.1 and SDG 11.2.1 in 2020. For SDG 9.1.1, the variables include rural population, rural population density, rural road density, rural mean elevation, rural slope standard deviation, and urban GDP. The MGWR model for SDG 11.2.1 included urban population, urban population density, urban slope standard deviation, urban public transport station density, urban mean elevation, and urban GDP. The model fit accuracy for SDG 9.1.1 was 0.824, indicating excellent fit, while for SDG 11.2.1, it was 0.434.

In the MGWR model (Table 3), the effect of rural population density, rural road density, rural mean altitude, and rural slope standard deviation on the SDG 9.1.1 indicators was significant according to the t-value (absolute value > 2 is significant) and *p*-value (*p*-value < 0.05 is significant). Rural road density and rural mean elevation were, respectively, the most significant positive and negative correlates affecting the SDG 9.1.1 indicator value. The variable estimate of rural road density was 0.428, which showed a positive correlation, i.e., for every one unit increase in road density per square kilometer, the indicator would increase by 0.428 units on average. The variable estimate of rural mean elevation was −0.608, which showed a negative correlation, i.e., for every one kilometer decrease in elevation, the indicator would decrease by 0.608 units. The SDG 9.1.1 indicator was significantly associated with both mean elevation and slope standard deviation, both negatively correlated, indicating that higher elevation or the more hilly terrain led to lower SDG 9.1.1 indicator values.

Table 3. SDG 9.1.1 statistical description of multi-scale geographically weighted regression coefficients.

Indicator	Variable	Estimated Value of Variables	Standard Error	t-Value	*p*-Value
SDG 9.1.1	Rural population	0.081	0.045	1.798	0.072
	Rural population density	−0.239	0.059	−4.017	0.000
	Rural road density	0.428	0.056	7.692	0.000
	Rural average elevation	−0.608	0.052	−11.733	0.000
	Rural slope standard deviation	0.122	0.045	2.696	0.007
	GDP	−0.081	0.046	−1.758	0.079

For the SDG 11.2.1 indicator (Table 4), urban population density, urban public transport station density, and GDP significantly influenced the indicator value, all positively correlated. Urban public transport station density had the greatest impact, with an average increase of 0.459 units in the indicator value for every unit increase in density. GDP and population density also showed positive correlations, indicating that the more economically developed and densely populated regions in China had higher SDG 11.2.1 indicator values. Within cities, the effects of both the mean elevation and standard deviation of the slope were small and insignificant, indicating that geography had less influence on the SDG 11.2.1 indicator. This was consistent with the fact that urban areas were basically located in areas with less slope and suitable elevation.

Table 4. SDG 11.2.1 statistical description of multi-scale geographically weighted regression coefficients.

Indicator	Variable	Estimated Value of Variables	Standard Error	t-Value	*p*-Value
SDG 11.2.1	Urban population	−0.146	0.122	−1.197	0.231
	Urban population density	0.181	0.056	3.249	0.001
	Urban slope standard deviation	0.020	0.050	0.389	0.698
	Urban average elevation	0.042	0.050	0.843	0.399
	Urban public transportation station Density	0.459	0.049	9.425	0.000
	GDP	0.288	0.119	2.414	0.016

5. Discussion

Despite high scores on key indicators, Chongqing faces significant challenges with road and public transport accessibility. As a large municipality, Chongqing has a relatively low percentage of urbanized areas (Figure 8a), resulting in many regions being classified as rural [55]. This unclear rural–urban demarcation increases the apparent rural population without changing the population with limited access to road transport. Consequently, the calculated SDG 9.1.1 indicator is high, although many disadvantaged groups still lack easy road access. Accurately defining rural–urban boundaries is critical for improving indicator calculation accuracy and needs to be addressed in future research.

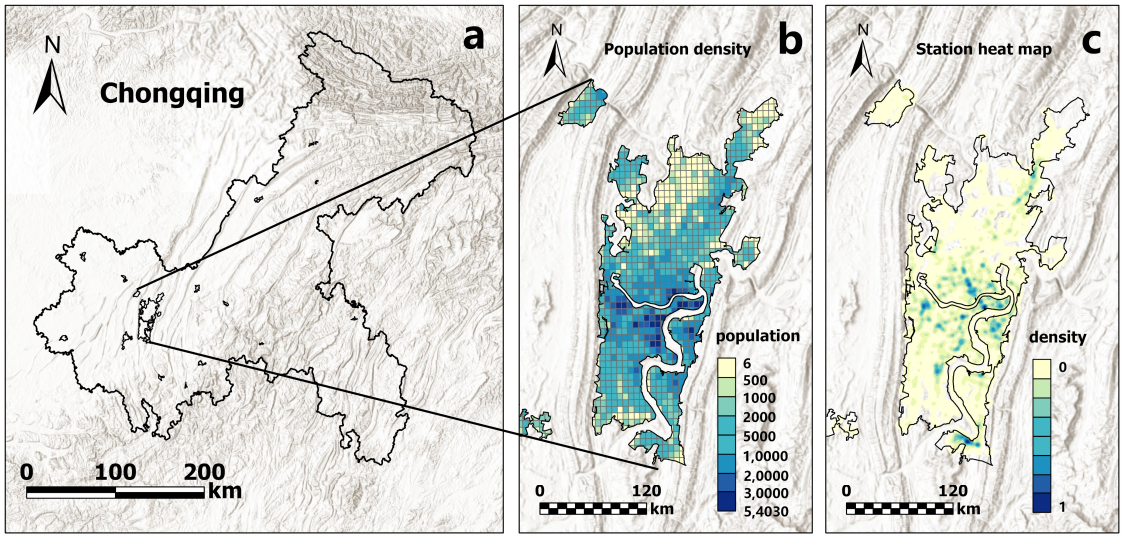


Figure 8. (**a**) shows the built-up area of Chongqing, (**b**) shows the population density of the built-up area and (**c**) shows the heat map of public transportation stations in the built-up area.

The further analysis of the built-up area's population density and public transport station heat maps (Figure 8b,c) showed that in the northern and southern parts of the built-up area, there was an insufficient coverage of public transport stations. Despite this, a high number of people live in these areas. Even where the coverage of smaller areas was lacking, there were multiple disadvantaged groups who found it very inconvenient to use public transport. The multivariate geographically weighted regression model indicates that public transport station density and population density are significant factors influencing this indicator. Therefore, government planning should fully consider these factors to improve public transport accessibility [56].

6. Conclusions

Utilizing the GEE platform, this study calculated and analyzed SDG 9.1.1 and SDG 11.2.1 indicators for 337 municipalities across China for the years 2015, 2020, and 2022. The study's key findings are as follows:

(i) The national average of SDG 9.1.1 in 2022 reached 99.36%, with an overall increase of 0.68% from 2015 to 2022. In 2015, the indicator exhibited a "high in the east and low in the west" distribution across the country, but it improved in the western region by 2022, with the lowest value at only 94.15%. The SDG 11.2.1 indicator reached 90.00% in 2022, an increase of 4.85%, with the indicator improving in the southeast coast and economically developed regions in 2015 and in many parts of the west by 2022.

(ii) China has continually improved road accessibility and public transport usage, reducing the number of disadvantaged groups for SDG 9.1.1 and SDG 11.2.1 by 52.2% and 25.3%, respectively, leaving approximately 1.89 million and 2.82 million disadvantaged individuals.

(iii) Spatial autocorrelation analysis showed higher SDG 9.1.1 indicator values in eastern China, with significant spatial aggregation, while SDG 11.2.1 indicator values exhibited high aggregation only in the Pearl River Delta, Yangtze River Delta, Sichuan, and Chongqing regions.

(iv) The multi-scale geographic regression model revealed rural road density and average rural altitude as significant factors influencing the SDG 9.1.1 indicator. For the SDG 11.2.1 indicator, urban population density, urban public transport station density, and GDP were significant factors.

This study provides crucial data support for enhancing transport infrastructure in China, a scientific basis for sustainable transport development, and a valuable reference for achieving the 2030 Sustainable Development Goals.

Author Contributions: M.Y.: conceptualization, methodology, formal analysis, writing—review and editing, visualization. Z.S.: conceptualization, methodology, supervision, funding acquisition. X.O.: writing—review and editing. H.L.: writing—review and editing, data curation. Y.H.: data curation, supervision. D.G.: writing—review and editing. All authors have read and agreed to the published version of the manuscript as written consent.

Funding: This research was supported by the National Key R&D Program of China (Project No. 2022YFC3800700), National Natural Science Foundation of China (grant number 42171291 and 42361144884), International Research Center of Big Data for Sustainable Development Goals (CBAS) (CBASYX0906), and Joint HKU-CAS Laboratory for iEarth (313GJHZ2022074MI, E4F3050300).

Data Availability Statement: The original contributions presented in the study are included in the article, further inquiries can be directed to the corresponding author.

Conflicts of Interest: The authors declare no conflicts of interest.

References

1. Bassi, A.M.; Pallaske, G.; Niño, N.; Casier, L. Does Sustainable Transport Deliver Societal Value? Exploring Concepts, Methods, and Impacts with Case Studies. *Future Transp.* **2022**, *2*, 115–134. [CrossRef]
2. Li, S.; Sun, Z.; Guo, H.; Ouyang, X.; Liu, Z.; Jiang, H.; Li, H. Localizing Urban SDGs Indicators for an Integrated Assessment of Urban Sustainability: A Case Study of Hainan Province. *Int. J. Digit. Earth* **2024**, *17*, 2336059. [CrossRef]
3. Friedman, J.; York, H.; Graetz, N.; Woyczynski, L.; Whisnant, J.; Hay, S.I.; Gakidou, E. Measuring and Forecasting Progress towards the Education-Related SDG Targets. *Nature* **2020**, *580*, 636–639. [CrossRef] [PubMed]
4. United Nations. Global Indicator Framework for the Sustainable Development Goals and Targets of the 2030 Agenda for Sustainable Development. 2021. Available online: https://unstats.un.org/sdgs/indicators/indicators-list/ (accessed on 26 June 2024).
5. Sachs, J.D.; Lafortune, G.; Fuller, G.; Drumm, E. *Implementing the SDG Stimulus. Sustainable Development Report 2023*; SDSN: Paris, France; Dublin University Press: Dublin, Ireland, 2023. [CrossRef]
6. Bennich, T.; Persson, Å.; Beaussart, R.; Allen, C.; Malekpour, S. Recurring Patterns of SDG Interlinkages and How They Can Advance the 2030 Agenda. *One Earth* **2023**, *6*, 1465–1476. [CrossRef]
7. Huang, C.; Feng, Y.; Wei, Y.; Sun, D.; Li, X.; Zhong, F. Assessing Regional Public Service Facility Accessibility Using Multisource Geospatial Data: A Case Study of Underdeveloped Areas in China. *Remote Sens.* **2024**, *16*, 409. [CrossRef]
8. Tiwari, G.; Phillip, C. Development of Public Transport Systems in Small Cities: A Roadmap for Achieving Sustainable Development Goal Indicator 11.2. *IATSS Res.* **2021**, *45*, 31–38. [CrossRef]
9. Liu, J.; Ji, L.; Sun, Y.; Chiu, Y.-H.; Zhao, H. Unleashing the Convergence Between SDG 9 and SDG 8 Towards Pursuing SDGs: Evidence from Two Urban Agglomerations in China During the 13th Five-Year Plan. *J. Clean. Prod.* **2024**, *434*, 139924. [CrossRef]
10. Saiu, V.; Blečić, I.; Meloni, I. Making Sustainability Development Goals (SDGs) Operational at Suburban Level: Potentials and Limitations of Neighbourhood Sustainability Assessment Tools. *Environ. Impact Assess. Rev.* **2022**, *96*, 106845. [CrossRef]
11. Jain, A.; Gue, I.H.; Jain, P. Research Trends, Themes, and Insights on Artificial Neural Networks for Smart Cities Towards SDG-11. *J. Clean. Prod.* **2023**, *412*, 137300. [CrossRef]
12. Snyman, L.; Coetzee, S. Measuring Geographic Accessibility in Data Poor Rural Areas by Augmenting the Road Network with a Triangular Irregular Network—A Case Study in the O.R. Tambo District Municipality of the Eastern Cape, South Africa. *J. Transp. Geogr.* **2024**, *115*, 103808. [CrossRef]
13. Qwaider, S.; Al-Ramadan, B.; Shafiullah, M.; Islam, A.; Worku, M.Y. GIS-Based Progress Monitoring of SDGs towards Achieving Saudi Vision 2030. *Remote Sens.* **2023**, *15*, 5770. [CrossRef]
14. Feng, Y.; Huang, C.; Song, X.; Gu, J. Assessing Progress and Interactions toward SDG 11 Indicators Based on Geospatial Big Data at Prefecture-Level Cities in the Yellow River Basin between 2015 and 2020. *Remote Sens.* **2023**, *15*, 1668. [CrossRef]

15. Jia, Z.; Wu, M.; Niu, Z.; Tang, B.; Mu, Y. Monitoring of UN Sustainable Development Goal SDG-9.1.1: Study of Algerian "Belt and Road" Expressways Constructed by China. *PeerJ* **2020**, *8*, e8953. [CrossRef] [PubMed]
16. Sun, Z.; Yu, S.; Guo, H.; Wang, C.; Zhang, Z.; Xu, R. Assessing 40 Years of Spatial Dynamics and Patterns in Megacities Along the Belt and Road Region Using Satellite Imagery. *Int. J. Digit. Earth* **2021**, *14*, 71–87. [CrossRef]
17. Guo, H.D. *Big Earth Data in Support of the Sustainable Development Goals (2023)*; Science Press and EDP Sciences: Beijing, China, 2023.
18. Osman, A.; Mensah, E.A.; Mensah, C.A.; Asamoah, Y.; Dauda, S.; Adu-Boahen, K.; Adongo, C.A. Spatial Analysis of Synergies and Trade-Offs Between the Sustainable Development Goals (SDGs) in Africa. *Geogr. Sustain.* **2022**, *3*, 220–231. [CrossRef]
19. LIU, Y.; LI, W.; ZHANG, X.; ZHANG, Y.; LI, R.; ZHOU, Q. Evaluating Rural Access Index Across China with Multi-source Open Data. J. *Geo-Inf. Sci.* **2023**, *25*, 783–793. [CrossRef]
20. Guo, H.D. *Big Earth Data in Support of the Sustainable Development Goals (2021)*; Science Press and EDP Sciences: Beijing, China, 2021.
21. Guo, H.; Liang, D.; Sun, Z.; Chen, F.; Wang, X.; Li, J.; Zhu, L.; Bian, J.; Wei, Y.; Huang, L.; et al. Measuring and Evaluating SDG Indicators with Big Earth Data. *Sci. Bull.* **2022**, *67*, 1792–1801. [CrossRef]
22. Han, L.; Lu, L.; Lu, J.; Liu, X.; Zhang, S.; Luo, K.; He, D.; Wang, P.; Guo, H.; Li, Q. Assessing Spatiotemporal Changes of SDG Indicators at the Neighborhood Level in Guilin, China: A Geospatial Big Data Approach. *Remote Sens.* **2022**, *14*, 4985. [CrossRef]
23. Liu, X.; Yuan, M. Assessing Progress Towards Achieving the Transport Dimension of the SDGs in China. *Sci. Total Environ.* **2023**, *858*, 159752. [CrossRef]
24. Zhao, Z.; Pan, Y.; Zhu, J.; Wu, J.; Zhu, R. The Impact of Urbanization on the Delivery of Public Service–Related SDGs in China. *Sustain. Cities Soc.* **2022**, *80*, 103776. [CrossRef]
25. Sharifi, A.; Allam, Z.; Bibri, S.E.; Khavarian-Garmsir, A.R. Smart Cities and Sustainable Development Goals (SDGs): A Systematic Literature Review of Co-benefits and Trade-offs. *Cities* **2024**, *146*, 104659. [CrossRef]
26. Workman, R.; McPherson, K. Measuring Rural Access for SDG 9.1.1. *Trans. GIS* **2021**, *25*, 721–734. [CrossRef]
27. Iimi, A.; Ahmed, F.; Anderson, E.C.; Diehl, A.S.; Maiyo, L.; Peralta-Quirós, T.; Rao, K.S. *New Rural Access Index: Main Determinants and Correlation to Poverty (English)*; Policy Research Working Paper, No. WPS 7876; World Bank Group: Washington, DC, USA, 2016; pp. 1–16. [CrossRef]
28. Ilie, C.M.; Brovelli, M.A.; Coetzee, S. Monitoring SDG9 with Global Open Data and Open Software: A Case Study from Rural Tanzania. *Int. Soc. Photogramm. Remote Sens.* **2019**, *42*, 1551–1558. [CrossRef]
29. Shi, F.; Zhu, L.; Yuan, R. Progress of Public Transport Accessibility Analysis Methods. *Hum. Geogr.* **2022**, *37*, 20–29.
30. Biba, S.; Curtin, K.M.; Manca, G. A New Method for Determining the Population with Walking Access to Transit. *Int. J. Geogr. Inf. Sci.* **2010**, *24*, 347–364. [CrossRef]
31. Thakuriah, P. Urban Transportation Planning: A Decision-Oriented Approach. *J. Transp. Eng.* **2001**, *127*, 454. [CrossRef]
32. Yigitcanlar, T.; Sipe, N.; Evans, R.; Pitot, M. A GIS-Based Land Use and Public Transport Accessibility Indexing Model. *Aust. Plan.* **2007**, *44*, 30–37. [CrossRef]
33. Silva, C.; Pinho, P. The Structural Accessibility Layer (SAL): Revealing How Urban Structure Constrains Travel Choice. *Environ. Plan. A* **2010**, *42*, 2735–2752. [CrossRef]
34. Papa, E.; Bertolini, L. Accessibility and Transit-Oriented Development in European Metropolitan Areas. *J. Transp. Geogr.* **2015**, *47*, 70–83. [CrossRef]
35. O'Sullivan, D.; Morrison, A.; Shearer, J. Using Desktop GIS for the Investigation of Accessibility by Public Transport: An Isochrone Approach. *Int. J. Geogr. Inf. Sci.* **2000**, *14*, 85–104. [CrossRef]
36. Burns, C.M.; Inglis, A.D. Measuring Food Access in Melbourne: Access to Healthy and Fast Foods by Car, Bus, and Foot in an Urban Municipality in Melbourne. *Health Place* **2007**, *13*, 877–885. [CrossRef] [PubMed]
37. Boisjoly, G.; Moreno-Monroy, A.I.; El-Geneidy, A. Informality and Accessibility to Jobs by Public Transit: Evidence from the São Paulo Metropolitan Region. *J. Transp. Geogr.* **2017**, *64*, 89–96. [CrossRef]
38. Qiu, Y.; Zhao, X.; Fan, D.; Li, S. Geospatial Disaggregation of Population Data in Supporting SDG Assessments: A Case Study from Deqing County, China. *Int. J. Geo-Inf.* **2019**, *8*, 356. [CrossRef]
39. Soldatke, N.; Sydorów, M.; Żukowska, S. Assessment of the Accessibility of Public Transport in the Tricity (Poland): Analytical Use of Geographical Information Systems (GIS) in the Context of Selected Public Transport Measures. *Int. J. Digit. Earth* **2024**, *17*, 2344–2586. [CrossRef]
40. Sun, Z.; Du, W.; Jiang, H.; Weng, Q.; Guo, H.; Han, Y.; Xing, Q.; Ma, Y. Global 10-m Impervious Surface Area Mapping: A Big Earth Data-Based Extraction and Updating Approach. *Int. J. Appl. Earth Obs. Geoinf.* **2022**, *109*, 102800. [CrossRef]
41. Gorelick, N.; Hancher, M.; Dixon, M.; Ilyushchenko, S.; Thau, D.; Moore, R. Google Earth Engine: Planetary-Scale Geospatial Analysis for Everyone. *Remote Sens. Environ.* **2017**, *202*, 18–27. [CrossRef]
42. Meng, L.; Li, Y.; Shen, R.; Zheng, Y.; Pan, B.; Yuan, W.; Li, J.; Zhuo, L. Large-Scale and High-Resolution Paddy Rice Intensity Mapping Using Downscaling and Phenology-Based Algorithms on Google Earth Engine. *Int. J. Appl. Earth Obs. Geoinf.* **2024**, *128*, 103725. [CrossRef]
43. Sun, L.; Lou, Y.; Shi, Q.; Zhang, L. Spatial Domain Transfer: Cross-Regional Paddy Rice Mapping with a Few Samples Based on Sentinel-1 and Sentinel-2 Data on GEE. *Int. J. Appl. Earth Obs. Geoinf.* **2024**, *128*, 103762. [CrossRef]
44. Goodchild, M.F. First Law of Geography. In *International Encyclopedia of Human Geography*; Kitchin, R., Thrift, N., Eds.; Elsevier: Oxford, UK, 2009; pp. 179–182. [CrossRef]

45. Oshan, T.M.; Li, Z.; Kang, W.; Wolf, L.J.; Fotheringham, A.S. MGWR: A Python Implementation of Multiscale Geographically Weighted Regression for Investigating Process Spatial Heterogeneity and Scale. *ISPRS Int. J. Geo-Inf.* **2019**, *8*, 269. [CrossRef]
46. Mikou, M.; Rozenberg, J.; Koks, E.E.; Fox, C.J.E.; Peralta Quiros, T. Assessing Rural Accessibility and Rural Roads Investment Needs Using Open Source Data; World Bank Policy Research Working Paper No. 8746. 2019. Available online: https://ssrn.com/abstract=3338184 (accessed on 26 June 2024).
47. Qiao, W.; Hu, B.; Guo, Z.; Huang, X. Evaluating the Sustainability of Land Use Integrating SDGs and Its Driving Factors: A Case Study of the Yangtze River Delta Urban Agglomeration, China. *Cities* **2023**, *143*, 104569. [CrossRef]
48. Ministry of Civil Affairs of the People's Republic of China. *2020 Statistical Bulletin on the Development of Civil Affairs*; Ministry of Civil Affairs of the People's Republic of China: Beijing, China, 2020. Available online: https://www.mca.gov.cn/images3/www2017/file/202109/1631265147970.pdf (accessed on 26 May 2024).
49. Firoiu, D.; Ionescu, G.H.; Cismaș, L.M.; Vochița, L.; Cojocaru, T.M.; Bratu, R.-Ș. Can Europe Reach Its Environmental Sustainability Targets by 2030? A Critical Mid-Term Assessment of the Implementation of the 2030 Agenda. *Sustainability* **2023**, *15*, 16650. [CrossRef]
50. Jiang, H.; Guo, H.; Sun, Z.; Xing, Q.; Zhang, H.; Ma, Y.; Li, S. Projections of Urban Built-Up Area Expansion and Urbanization Sustainability in China's Cities Through 2030. *J. Clean. Prod.* **2022**, *367*, 133086. [CrossRef]
51. Jiang, H.; Sun, Z.; Guo, H.; Xing, Q.; Du, W.; Cai, G. A Standardized Dataset of Built-Up Areas of China's Cities with Populations Over 300,000 for the Period 1990–2015. *Big Earth Data* **2022**, *6*, 103–126. [CrossRef]
52. Jiang, H.; Sun, Z.; Guo, H.; Weng, Q.; Du, W.; Xing, Q.; Cai, G. An Assessment of Urbanization Sustainability in China Between 1990 and 2015 Using Land Use Efficiency Indicators. *NPJ Urban Sustain.* **2021**, *1*, 34. [CrossRef]
53. Bivand, R.; Müller, W.G.; Reder, M. Power Calculations for Global and Local Moran's. *Comput. Stat. Data Anal.* **2009**, *53*, 2859–2872. [CrossRef]
54. Li, L.; Cai, J.; Chen, W. How Does Transport Development Contribute to Rural Income in China? Evidence from County-Level Analysis Using Structural Equation Model. *Travel Behav. Soc.* **2024**, *34*, 100708. [CrossRef]
55. Liu, R.; Zhang, L.; Tang, Y.; Jiang, Y. Understanding and Evaluating the Resilience of Rural Human Settlements with a Social-Ecological System Framework: The Case of Chongqing Municipality, China. *Land Use Policy* **2024**, *136*, 106966. [CrossRef]
56. Gao, L.; Chong, H.-Y.; Zhang, W.; Li, Z. Nonlinear Effects of Public Transport Accessibility on Urban Development: A Case Study of Mountainous City. *Cities* **2023**, *138*, 104340. [CrossRef]

Disclaimer/Publisher's Note: The statements, opinions and data contained in all publications are solely those of the individual author(s) and contributor(s) and not of MDPI and/or the editor(s). MDPI and/or the editor(s) disclaim responsibility for any injury to people or property resulting from any ideas, methods, instructions or products referred to in the content.